

Fully Bio-Based Epoxy Thermoset Based on Epoxidized Linseed Oil and Tannic Acid

Nikita Reinhardt, Jonas M. Breitsameter, Klaus Drechsler, and Bernhard Rieger*

Increasing demand for bio-based epoxy thermoset alternatives has risen in the last few years. Epoxidized vegetable oils (EVO) have attracted significant attention due to their bio-based, unharmed nature and high availability. This study proposes a fully bio-based epoxy thermoset based on epoxidized linseed oil (ELO) and tannic acid (TA). TA allows, with its high degree of functionality and aromatic structure as a curing agent for ELO, to create a fully bio-based polymer network with a high glass transition temperature (T_g), high stiffness, and high strength. A maximum T_g of 146 °C, a flexural modulus of 2986 MPa, and flexural strength of 72 MPa are obtained. The strong material properties of the TA/ELO thermoset expose its potential as a bio-based substitute for petrochemical-based epoxy resins for high-performance applications.

1. Introduction

Epoxy thermosets (EP) are well established in a large variety of applications, including electronic encapsulation, paints, coatings, adhesives, sealants, and composite materials. EPs represent a prominent place in the thermosetting market. Its market is expected to witness further growth in the forecast period of 2021–2026, growing at a Compound Annual Growth rate (CAGR) of 5%, and is projected to reach ≈ 4.3 million metric tons by 2026.^[1]

About 90% of the epoxy thermoset is derived from diglycidyl ether of bisphenol A (DGEBA). The raw materials for DGEBA, bisphenol A (BPA), and epichlorohydrin (ECH) are petroleum-based and cause adverse effects on living organisms and ecosystems. Glycerol, a byproduct from the biodiesel industry, can be used to produce ECH. However, considerable

research has been and is still being focused on using bio-based compounds to replace BPA, which is classified as an endocrine disruptor.^[2,3a–h,4,5] Moreover, some commonly used curing agents such as polyamine, polyamide, and anhydride hardeners are toxic before curing. Additionally, toxicity in cured epoxy materials may not be avoided as incomplete consumption of curing agents may remain.^[2,6,7] As a result, there is an increasing demand for bio-based epoxy thermoset alternatives.

Epoxidized vegetable oils (EVO) such as epoxidized soybean oil (ESO), epoxidized canola oil, or epoxidized linseed oil (ELO) have attracted great attention as

an epoxy resin replacement due to their bio-based, unharmed nature, high availability, and relatively low price.^[8,9] However, EVOs have drawbacks. Their long aliphatic chains impart flexibility, and the location of their oxirane rings in non-terminal positions is responsible for their lower reactivity than conventional DGEBA epoxy resins, which limit their practical use in structural applications.^[9,10–12] Generally, the mechanical and thermal properties of EPs depend strongly on their chemical structures, which are determined by the types of epoxy resins and curing agents used. ELO is the most suitable EVO for high-performance applications due to its high amount of epoxy groups in its linolenic acid chain.^[10,12,13] Due to the flexible structure of the triglycerides in the epoxidized linseed oil, a hardener with a rigid chemical structure is needed to create a thermoset that exhibits high stiffness and strength. A hardener with a rigid structure such as an aromatic ring structure is, therefore, more suited than a hardener with a long aliphatic chain to obtain a stiff and highly crosslinked network with ELO.^[14,15] Finding a bio-based, nontoxic, and non-harmful hardener capable of creating rigid networks with ELO to use bio-based thermosets in high-performance applications is of high interest. Biologically sourced and nontoxic hardeners used industrially are quite rare as their synthesis and isolation mechanisms are complex and constrain their commercialization. Furthermore, the T_g of the epoxy cured with a bio-based hardener is often too low for high-performance application.^[2,6]

A particular focus is given in this publication to the bio-sourced tannic acid (TA). TA is a nontoxic polyphenolic compound found in nuts, galls, seeds, and tree bark, and is affirmed as generally recognized as safe (GRAS).^[6,16,17] TA has potentially 25 galloyl hydroxyl groups capable of cross-linking, and the rigid gallic structure suggests the formation of highly crosslinked networks and strong mechanical properties. TA has the advantage of being already industrially isolated and an inexpensive chemical. The high potential of TA as a bio-based substitute for

N. Reinhardt, K. Drechsler
TUM School of Engineering and Design
Chair of Carbon Composites
Technical University of Munich
Boltzmannstr. 15, 85748 Garching, Germany

J. M. Breitsameter, B. Rieger
TUM Department of Chemistry
Wacker-Chair of Macromolecular Chemistry
Technical University of Munich
Lichtenbergstr. 4, 85748 Garching, Germany
E-mail: rieger@tum.de

 The ORCID identification number(s) for the author(s) of this article can be found under <https://doi.org/10.1002/mame.202200455>

© 2022 The Authors. Macromolecular Materials and Engineering published by Wiley-VCH GmbH. This is an open access article under the terms of the Creative Commons Attribution License, which permits use, distribution and reproduction in any medium, provided the original work is properly cited.

DOI: 10.1002/mame.202200455

petrochemical-based and toxic curing agents has already been highlighted, and several studies have been carried out to generate epoxy thermosets from TA. Shibata et al. used commercial TA as a curing agent to prepare EP with glycerol polyglycidylether (GPE) and sorbitol polyglycidylether (SPE).^[18] TA as an alternative curing agent for the commercially available DGEBA has also been investigated.^[17,19] Korey et al. found for the DGEBA cured with TA thermoset a $T_g > 200$ °C, which is within the range of several commercially available high T_g EPs, such as dicyandiamide and 4,4'-diaminodiphenyl sulfone.^[6] The use of TA to cure EVO has also been researched. Qi et al. cured ESO with tannic acid to obtain fully bio-based EP. However, only moderate thermal and mechanical properties were obtained such as a maximum T_g of 77 °C and a storage modulus of 1103 MPa at 25 °C.^[5]

Most of the studies that used TA as a curing agent were confronted with the issue of the low compatibility of TA in the resin. Solvents such as ethanol were used to dissolve TA in the resin, or TA was mixed in the resin at elevated temperatures to obtain a good homogeneous mixture. Elevated temperatures were finally applied to cure the thermoset.^[5,6,17,20] The use of solvents in epoxy thermosets has its drawbacks as removal is time-consuming and laborious, making the processing of the material challenging. Moreover, residues of solvent in the material can have a negative impact on the final properties of the epoxy.^[4,21] Furthermore, an elevated mixing and curing temperature is undesired for bio-based epoxies as it affects the carbon footprint of the end material, hinders its usage in low-temperature applications, and significantly impacts the pot-life of the material.

The main objective of the present study is to develop a fully bio-based epoxy thermoset from ELO and TA that does not contain any harmful substances and exhibits high stiffness, high strength, and high glass transition temperature with moderate curing temperatures. By milling TA into a fine powder, the use of solvents to dissolve TA in ELO could be avoided as TA could finely disperse in ELO to obtain a thermoset with strong thermal and mechanical properties.

2. Experimental Section

2.1. Materials

The curing agent TA with a molecular weight of 1701.20 g mol⁻¹ was purchased from Sigma-Aldrich (Taufkirchen, Germany) as well as formic acid and hydrogen peroxide (35%). The bio-based air release additive Epinal EL 12.42 was bought from bto epoxy GmbH (Amstetten, Austria). Linseed oil was purchased from a local commercial source and used for the synthesis of epoxidized linseed oil without further purification. The oil was cold-pressed, unprocessed, and of food-grade quality. The acid number was determined by the procedure of ISO 660.2009 to be 0.93 mg KOH per gram and the iodine value 186 g(I₂) per 100 g (ISO 3961.2018).

2.2. Synthesis of Epoxidized Linseed Oil

The epoxidation of linseed oil was carried out by the in situ generation of performic acid from formic acid and hydrogen peroxide. Before the epoxidation reaction, the average amount of double bonds per triglyceride was determined by ¹H-NMR (Fig-

ure S1, Supporting Information) to be ≈6.2. For the average molar weight of linseed oil, the value of 878 g mol⁻¹ was taken from the literature.^[21] The ratio of linseed oil to formic acid to hydrogen peroxide was 1.0:1.0:10. The reaction was performed in a double-wall 2 L glass reactor connected to a thermostat for cooling or heating, respectively. The linseed oil (422 g, 0.479 mol) was loaded into the reaction vessel. Hydrogen peroxide (411.8 mL, 4.79 mol, 35 %) was added, the mixture was stirred with a glass overhead KPG-stirrer (400 rpm), and the reactor was cooled to 10 °C. Formic acid (18.60 mL, 22.04 g, 0.479 mol) was added dropwise for 30 min, and then the temperature was raised to 50 °C. The epoxidation progress was monitored by ¹H-NMR spectroscopy (Figure S2, Supporting Information), and the reaction was finished within 48 h. After cooling the reaction mixture to room temperature, it was neutralized by adding a saturated sodium bicarbonate solution (200 mL) and diluted with diethyl ether (200 mL). After washing with a saturated sodium chloride solution, the solvent was removed in vacuo.

The EEW was estimated to be 140.6 g mol⁻¹ resulting from the molecular weight of linseed oil (878 g mol⁻¹) and ≈6.2 double bonds per triglyceride determined by ¹H-NMR analysis.^[22] The conversion toward the epoxide is determined to be > 99 % since there is no residual signal of the double bond in ¹H-NMR (Figure S2, Supporting Information) visible.

2.3. Milling of Tannic Acid

Obtaining a finely dispersed and homogenous TA/ELO mixture with excellent quality is of high importance to obtain good mechanical and thermal properties. To properly disperse TA into ELO without using any solvents, TA particle size must be reduced significantly. Thus, TA was milled with aluminum hydroxide (Al₂O₃) balls in a two-step milling process. First, TA was dried in a vacuum oven at 105 °C for 2 h. One hundred grams of dried TA, together with 40 Al₂O₃ balls with a diameter of 10 mm and 40 Al₂O₃ balls with a diameter of 5 mm, were placed inside an aluminum container of 1000 mL. The container was placed inside a speed mixer DAC-3000 HP (Hauschild GmbH & Co. KG, Germany), and a pre-milling was performed at a rotation speed of 650 rpm for 3 min. Four grinding cycles were applied. TA was cooled down to room temperature for 15 min between every grinding cycle. The gained powder was then dried again at 105 °C under vacuum for 2 h to remove the released water, cooled down to room temperature, and four more grinding cycles were applied. As a second step, the pre-milled TA powder, together with the Al₂O₃ balls, was put inside a 3D shaker mixer by Willy A. Bachofen AG (Switzerland). Milling at a speed of 50 rpm was then performed for 16 h. At last, the fine TA powder was separated from the grinding balls by a coarse meshed stainless-steel sieve and dried under vacuum at 105 °C for 4 h. The particle size of TA was reduced significantly after the two-step milling process, as shown in **Figure 1**. **Figure S3** (Supporting Information) shows how a fine particle size helps to obtain a better TA dispersion in ELO.

2.4. Epoxy Sample Preparation

TA/ELO epoxy samples with a molar ratio –OH/epoxide of 0.85, 1.0, 1.15, 1.25, 1.5, 1.75, and 2.0 were prepared to investigate the

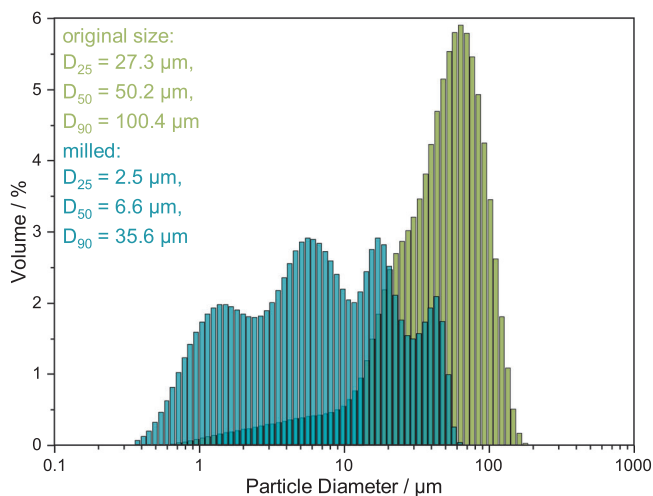


Figure 1. Particle size distribution of original size TA (as bought) and milled TA.

Table 1. Mixing ratios for the prepared TA/ELO samples.

| Samples | ELO [g]: TA[g] | Molar ratio R [-OH/epoxide] |
|-------------|----------------|-----------------------------|
| TA/ELO 0.85 | 100:41.14 | 0.85 |
| TA/ELO 1.0 | 100:48.40 | 1.0 |
| TA/ELO 1.15 | 100:55.66 | 1.15 |
| TA/ELO 1.25 | 100:60.50 | 1.25 |
| TA/ELO 1.5 | 100:72.60 | 1.5 |
| TA/ELO 1.75 | 100:84.70 | 1.75 |
| TA/ELO 2.0 | 100:96.80 | 2.0 |

influence of the molar ratio on the curing behavior and the thermal and mechanical properties of the thermoset. The samples were prepared as follows: 50 g of ELO and the corresponding amount of the finely milled and dried TA powder and 0.5 wt% of the air release additive (Epinal EL 12.42 bto epoxy GmbH) were placed in a 500 mL aluminum container. The mixing ratios are given in **Table 1**. Epinal EL 12.42 is a surface active polyether siloxane with a certified biobased-carbon content that facilitates the removal of air inclusion and does not participate in the curing reaction. The container was placed inside a speed mixer DAC-3000 HP (Hauschild GmbH & Co. KG, Germany) and sealed with a vacuum. Mixing of the components was performed at a rotation speed of 600 rpm for 10 min. The mixture was then poured into the cavities of an aluminum mold. The cavities had the dimensions 60 mm × 6 mm × 2 mm (for Dynamic Mechanical Analysis; DMA) and 80 mm × 10 mm × 4 mm (for flexural testing). Teflon tape was applied inside the cavities to ensure easy removal of the samples after curing. The mold was placed in a vacuum oven to remove air inclusions with a temperature of 80 °C and a pressure of 1 mbar for 2 h. Finally, the mold was placed in a standard oven for curing. All the TA/ELO samples listed in **Table 1** were prepared once with the curing condition C1: 16 h at 90 °C + 3 h at 140 °C and once with the curing condition C2: 16 h at 120 °C + 3 h at 140 °C (**Table 2**) to investigate the impact of the curing temperature on the thermal and mechanical properties of the var-

Table 2. Curing conditions for the TA/ELO samples.

| Curing condition | Curing time + temperature | Post-curing time + temperature |
|------------------|---------------------------|--------------------------------|
| C1 | 16 h at 90 °C | 3 h at 140 °C |
| C2 | 16 h at 120 °C | 3 h at 140 °C |

ious TA/ELO samples. After curing, the edges of the samples were wet-polished with sandpaper (grit size 500) for a smooth finish.

2.5. Characterization

2.5.1. Differential Scanning Calorimetry (DSC)

DSC was performed on unreacted ELO/TA mixtures with a Q2000 Differential Scanning Calorimeter (TA Instruments, USA). Five grams of ELO and the corresponding amount of milled TA were put inside small plastic containers of 50 mL and mixed for 3 min inside a speed mixer DAC 150 SP by Hauschild Engineering (Germany) at a rotation speed of 1500 rpm. Five to seven milligrams of the TA/ELO mixture were loaded inside a TZero aluminum pan and sealed with a TZero Hermetic lid from TA Instruments. Thermograms of the various TA/ELO formulations were recorded between 23 and 320 °C under a nitrogen atmosphere (gas flow = 50 mL min⁻¹). The applied heating rate was 10 K min⁻¹. The temperature of the peak of the curing enthalpy was determined with the Software Universal Analysis. Three thermograms were recorded for each TA/ELO formulation. Thermograms of the neat, milled, and dried TA were also recorded.

2.5.2. Dynamic Mechanical Analysis (DMA)

DMA measurements were performed using a DMA Q800 (TA Instruments, US) under a nitrogen atmosphere with a 20 mm 3-point bending clamp. The TA/ELO specimens of dimensions 60 mm × 6 mm × 2 mm were cut lengthwise into two to have the dimensions 30 mm × 6 mm × 2 mm. After being dried for 3 days in a vacuum chamber with silica balls, the samples were subjected to an oscillating flexural load with an amplitude of 80 μm, a frequency of 10 Hz, a static pre-load of 0.01 N, and a force profile of 125%. During loading, the samples were first equilibrated at -20 °C for 15 min, then a temperature ramp of 1 K min⁻¹ was applied up to 180 °C. Two specimens were characterized for each TA/ELO sample cured with C1 and C2. The glass transition temperature T_g was identified as the temperature of the peak of the tan δ curve using the software Universal Analysis.

2.5.3. Flexural Testing

TA/ELO samples of dimensions 80 mm × 10 mm × 4 mm were first dried for 3 days in a vacuum chamber with silica balls before testing. Three-point bending Flexural testing was performed with a universal testing machine Inspekt 250 (Hegewald & Peschke,

Germany) according to DIN EN ISO 178. The force was measured using a 500 N load cell. The tests were performed at a constant loading speed of 2 mm min⁻¹ with a span of 64 mm, and stress/strain curves were recorded. The flexural modulus was evaluated from the stress/strain curve in the elongation range between 0.05 and 0.25 %. Flexural strength and elongation at break were also evaluated. Five specimens were tested for each TA/ELO sample cured with C1 and C2. The laboratory temperature and humidity during testing were 21.6 °C and 36 %.

2.5.4. Optical Microscopy

After flexural testing, TA/ELO samples were placed in a cylindrical form, embedded with epoxy CR80 from SIKA, and cured at 55 °C for 16 h. The specimens were then polished with a polishing machine, and the morphology of the fracture surface was analyzed with an optical microscope BX41M-LED (Olympus, Germany). Unmilled and milled TA, neat and dispersed in ELO, were also analyzed.

2.5.5. Nuclear Magnetic Resonance (NMR) Spectroscopy

¹H-NMR spectra of natural linseed oil and ELO were recorded on a Bruker Ascend 400 MHz spectrometer. All spectra are referenced on the proton signal of CDCl₃ (7.26 ppm).

2.5.6. Thermogravimetric Analysis (TGA)

TGA Q5000, (TA Instruments, US) was used to conduct thermogravimetric analyses on TA/ELO samples cured with C2, on neat TA and ELO. One to two milligrams of samples are heated from 23 to 1000 °C with a heating rate of 10 K min⁻¹ under an argon atmosphere. Analysis of the mass loss in dependency of temperature is performed using TA universal software. The temperature *T*_{5%} at a weight loss of 5 % of the various samples was determined.

2.5.7. Particle Size Analysis

The particle size distribution of the milled and unmilled TA was determined by an LS 13 320 laser diffraction particle size analyzer (Beckman Coulter, US) using the Tornado dry powder system and the Mie optical model.

2.5.8. Water Absorption

TA/ELO specimens of dimensions 30 mm × 6 mm × 2 mm cured with C2 were dried in a vacuum oven at 50 °C for 14 days and weighed. The samples were then immersed in distilled water at 23 °C. After 7 days, the samples were wiped and weighed.

2.5.9. Gel Content

Gel contents of the cured and dried TA/ELO samples were determined by Soxhlet extraction for 24 h using ethanol. The extracted samples were dried in a vacuum oven at 55 °C until weight constancy.

2.5.10. Attenuated Total Reflection Fourier Transformed Infrared Spectroscopy (ATR-FTIR)

ATR-FTIR measurements were performed on a Bruker Vertex 70v ATR-IR spectrometer at room temperature in absorption mode. Signal intensities were normalized to the C=C vibration band of TA (1610 cm⁻¹).

3. Results and Discussion

3.1. Curing Mechanism of TA/ELO Epoxy

Unlike other widely used curing agents, curing with phenolic curing agents such as TA is more complex in terms of curing mechanism. TA, as shown in **Figure 2b**) contains 25 hydroxyl groups capable of reacting with epoxy groups of the ESO. However, due to steric hindrance effects during the curing process and low reactivity of the galloyl groups, the participation of every single hydroxyl functionality in the curing reaction is very unlikely.^[17] The curing reaction follows a ring-opening mechanism of the oxirane group described by Qi et al. as a zwitterionic pathway. The alcohol group coordinates with the epoxide forming a hydrogen-bridge linkage (**Figure 2a**). This allows the nucleophilic attack of the alcohol oxygen to an epoxide carbon leading to a zwitterionic species and subsequently to the ring-opening and ether bond formation.^[5] The formed network is schematically shown in **Figure 2b**).

To better understand the reaction between TA and ELO, an exemplary DSC heating scan of TA/ELO 1.75 is shown in **Figure 3A**). All the DSC scans conducted have similar shapes, and three distinguished areas can be identified. First, an endothermic peak ranging approximately from 25 to 100 °C corresponding to the evaporation of hydrated water can be seen (**Figure 3A(I)**). The presence of water despite the drying procedure can be confirmed by the DSC and TGA scan of the neat, milled, and dried TA. The TGA scan shows a mass loss of 1.7 % at 120 °C whereas the DSC scan shows an endothermic process ranging approximately from 25 to 120 °C (**Figure 3B**; **Figure S4**, Supporting Information). After one day exposed to the laboratory atmosphere (55% humidity, 25 °C), the TGA measurement was repeated and showed a mass loss of 9.1 % at 120 °C that shows the hygroscopic behavior of TA (**Figure S4**, Supporting Information). Second, an exothermic peak corresponding to the reaction between phenolic –OH groups and the epoxides starting at ≈100 °C and ending at ≈250 °C is observed (**Figure 3A(II)**). This is in accordance with previous literature as the reaction between phenolic –OH groups and epoxy rings can already occur at a temperature of 100 °C.^[6,17,23] With an increasing amount of TA, the temperature of the maximum of the exothermic peak shifts to lower temperatures (**Figure 3C**). Hence, with an excess of TA, the highest curing reaction speed is reached at lower temperatures, improving the curing efficiency. This observation could be explained by the high molar mass and the great steric hindrance of TA. After the formation of a few ether bonds during the initial curing period, the basic structure of the epoxy network is already defined. This results in a large proportion of potential hydroxy linking positions that do not contribute to network linking. Therefore, increasing the amount of TA leads to a higher possibility for the galloyl-groups to access regions with unreacted oxiranes, increasing the over-

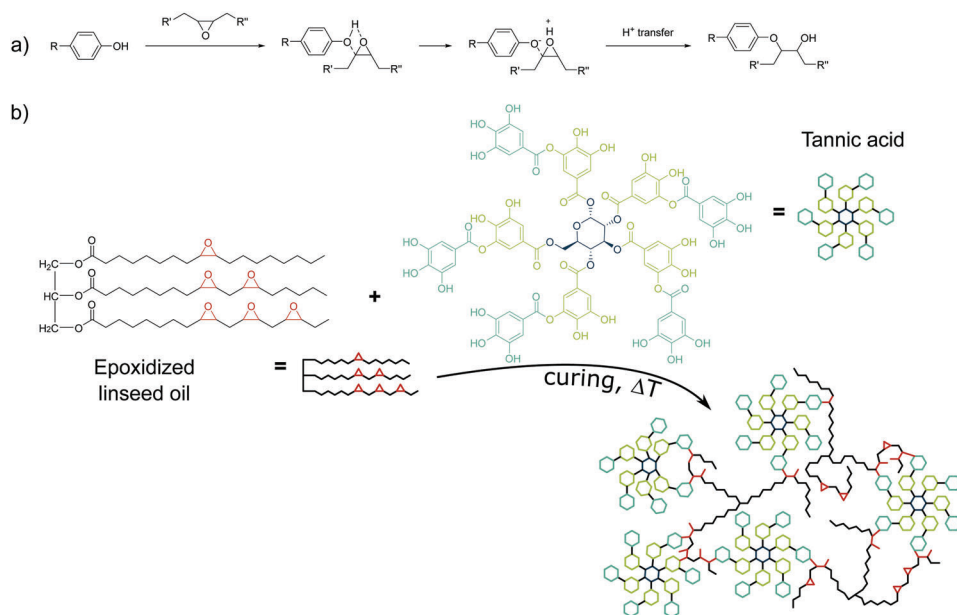


Figure 2. a) Curing mechanism following a zwitterionic ring-opening reaction exemplary shown on a phenol group according to Qi et al.^[5] b) Schematic formation of a 3D network during the curing reaction.

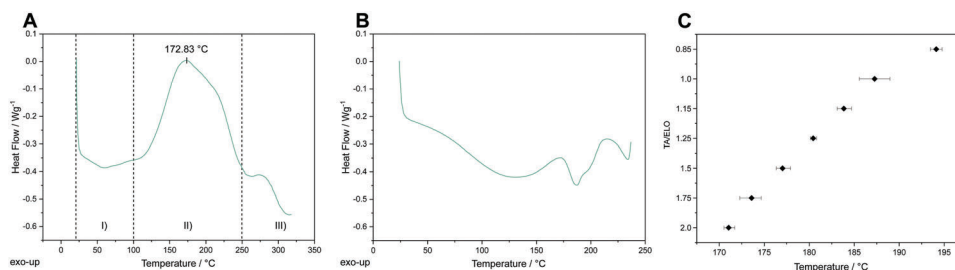


Figure 3. A) DSC scan of the sample TA/ELO 1.75. The temperature of the peak of the curing enthalpy: 172.83 °C, B) DSC scan of neat, milled, and dried TA, C) Average temperature of the peak of the curing enthalpy for the different TA/ELO mixtures.

all degree of cross-linking. Finally, a shoulder in the DSC scan (Figure 3A(III)) >250 °C, linked with the degradation of TA and confirmed with the TGA scan of neat TA (Figure 8), is observed. The shoulder becomes more distinctive with an excess of TA as more TA particles cannot participate in the curing reaction and cross-link with ELO, and hence, start degrading (Figure S5, Supporting Information).

3.2. Thermo-Mechanical Properties

The curing conditions C1 and C2 were chosen after preliminary investigations. To begin with, different pre-curing temperatures were investigated. 120 °C corresponds to the approximate onset temperature of the curing enthalpy of TA/ELO (Figure S6, Supporting Information). Samples cured with a higher pre-curing temperature (140 °C) had a higher stiffness. However, the samples were extremely brittle as flexural strength and elongation at break were significantly lower (Table S1, Supporting Information). Therefore, the pre-curing temperature was set at 120 °C. As a low curing temperature allows saving energy and easier

processing, the pre-curing temperature of 90 °C was also chosen to see if good mechanical and thermal properties could be achieved with a low curing temperature. A post-curing is usually needed to maximize the thermal and mechanical properties of epoxy thermosets and it is commonly set at a higher temperature than the applied pre-curing temperature.^[24] DMA tests showed that a post-curing at 140 °C helped increase the stiffness and T_g of the TA/ELO thermoset.

Thermo-mechanical properties and T_g of the different TA/ELO samples were analyzed by DMA, which is a very sensitive technique for measuring glass transition temperatures.^[25] T_g is an essential indicator for EPs. It defines the temperature range at which EP can be used in high-performance structural applications as above T_g ; they are visco-elastic and soft materials. **Figure 4** depicts the variations of storage modulus, loss modulus, and $\tan \delta$ for the sample TA/ELO 1.75 cured with C1. Similar curves were obtained for all other samples, and broad $\tan \delta$ peaks were observed. A wide $\tan \delta$ peak can be a characteristic of the relaxation of a heterogeneous network.^[26] However, in the case of the TA/ELO thermoset, a broad $\tan \delta$ is a consequence of the complex crosslinked structure formed. Unlike standard

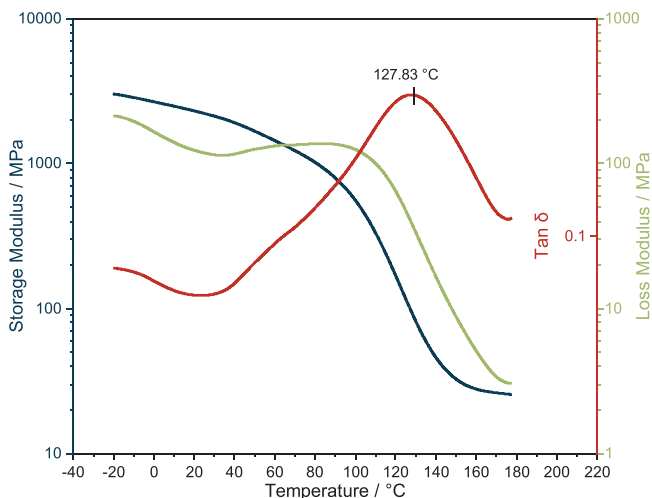


Figure 4. Characterization of the thermo-mechanical properties with DMA: storage modulus, loss modulus, and $\tan \delta$ variations versus temperature for the sample TA/ELO 1.75 cured with C1. T_g of 127.83 °C.

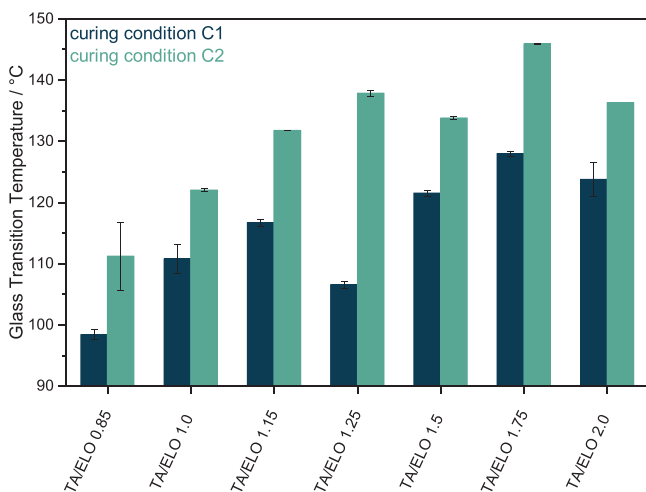


Figure 5. T_g obtained from DMA for the different TA/ELO samples cured with curing conditions C1 and C2.

epoxy compounds such as DGEBA, where oxirane groups are located at a fixed position, cross-linking in the case of ELO is not as straightforward. In fact, the oxirane groups are statistically distributed across the aliphatic triglyceride backbone of ELO.^[27] In addition, TA has a high molecular weight and the reactivity of the 25 hydroxy groups of TA is not equal and changes throughout the curing reaction due to steric and electronic effects.^[6] Therefore, cross-linking between ELO and TA leads to a complex and unpredictable network structure, broadening the glass transition.

It is typical for EPs that T_g is influenced by the epoxy and curing agent monomer ratio as the cross-linking density and structure vary.^[19] **Figure 5** gathers the T_g obtained for the different TA/ELO samples cured with C1 and C2. A clear trend can be seen as the T_g of all samples increases significantly when a curing temperature of 120 °C (curing condition C2) instead of 90 °C (condition C1) is applied. Therefore, the samples cured with C1 did not reach their full cross-linking potential. This could be confirmed

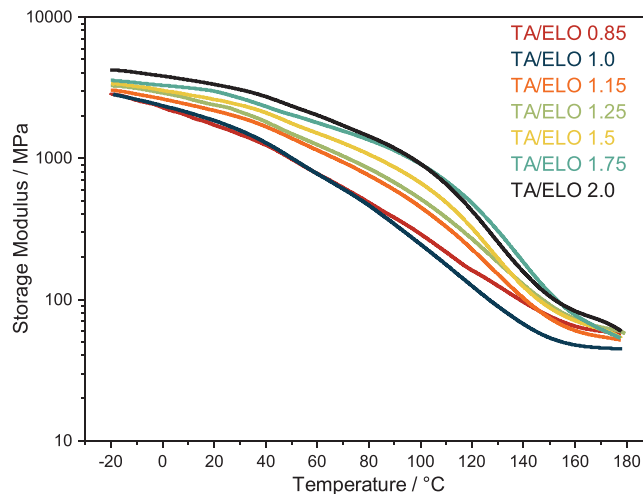


Figure 6. Comparison of the storage modulus curves (E') for the different TA/ELO samples cured with C2.

with the gel content measurements as the samples cured with C1 showed a lower Soxhlet degree of cross-linking than the samples cured with C2 (Figure S7, Supporting Information). As the curing process occurs at a temperature below the T_g of the fully cured resin ($T_{g\infty}$), the system vitrifies, and the reaction becomes diffusion controlled.^[28] Due to the vitrification and the additional low reactivity of the polyphenol groups in TA and steric hindrance of the epoxy groups along the fatty chains of ELO, a high curing temperature favors a higher cross-linking of the polymer chains. Significantly higher glass transition temperatures are also observed when the TA molar ratio exceeds 1.0. As already noticed with the DSC analysis, an excess of TA allows more efficient curing. This can also be seen with ATR-FTIR (Figures S8 and S9, Supporting Information). While TA/ELO 0.85 shows a residual signal of the C–O epoxide vibration at 820 cm^{-1} , it cannot be observed for samples with an excess of TA.^[29] Higher T_g was also observed in literature for TA-based thermosets when the TA molar ratio was increased.^[6,20] In our case, a maximum T_g of 146 °C was obtained for TA/ELO 1.75 cured with C2. One can also see in **Figure 5** that the T_g is not varying significantly between the samples TA/ELO 1.15, 1.25, 1.5, 1.75, and 2.0 cured with C2. This behavior can be the result of the complex crosslinked structure formed and the broadened glass transition. Furthermore, the fundamental network is already set within a few reactions. Several equations such as DiBenedetto's equation correlating T_g and the cross-linking of epoxies can be found in the literature.^[30] As TA is added in excess, all the oxiranes are able to interact with a galloyl-group and the cross-linking cannot vary much anymore (Figures S8 and S9, Supporting Information).

The storage modulus (E') is a measure of the sample's elastic behavior and is associated with stiffness.^[31] Studying the evolution of E' with the temperature is an excellent method to compare the stiffness of different samples at various temperatures. **Figure 6** depicts the evolution of E' with temperature for the different TA/ELO samples cured with C2. As expected, the TA/ELO thermoset's stiffness increases with the TA amount as a highly crosslinked structure is built. A maximum average storage modulus of 3218 MPa at ambient temperature (25 °C)

Table 3. Average Flexural Modulus, Flexural strength, and elongation at break obtained for the different TA/ELO mixtures cured with the curing conditions C1 and C2.

| Sample ↓ / Curing → | Flexural Modulus [MPa] | | Flexural Strength [MPa] | | Elongation at break [%] | |
|---------------------|------------------------|------------|-------------------------|--------|-------------------------|-----------|
| | C1 | C2 | C1 | C2 | C1 | C2 |
| TA/ELO 0.85 | 924 ± 91 | 1347 ± 94 | 33 ± 2 | 46 ± 2 | 8.2 ± 0.9 | 7.8 ± 0.8 |
| TA/ELO 1.0 | 1484 ± 131 | 1525 ± 105 | 48 ± 2 | 50 ± 2 | 8.4 ± 1.7 | 5.9 ± 0.3 |
| TA/ELO 1.15 | 1711 ± 43 | 2111 ± 98 | 50 ± 3 | 67 ± 1 | 4.9 ± 1.5 | 4.7 ± 0.3 |
| TA/ELO 1.25 | 1692 ± 59 | 1991 ± 27 | 50 ± 1 | 65 ± 1 | 4.9 ± 0.7 | 4.2 ± 0.5 |
| TA/ELO 1.5 | 1943 ± 157 | 2308 ± 99 | 54 ± 2 | 72 ± 1 | 3.7 ± 0.6 | 3.7 ± 0.1 |
| TA/ELO 1.75 | 2328 ± 257 | 2525 ± 187 | 63 ± 8 | 67 ± 6 | 2.8 ± 0.7 | 3.0 ± 0.3 |
| TA/ELO 2.0 | 2686 ± 158 | 2986 ± 42 | 45 ± 8 | 66 ± 3 | 1.8 ± 0.4 | 2.5 ± 0.1 |

was obtained for TA/ELO 2.0 cured with C2 (Figure S10, Supporting Information).

Regarding literature, the storage modulus and the T_g of the developed TA/ELO systems are high for EVO cured with bio-based curing agents. Todorovic et al. found a maximum storage modulus of 1380 MPa at 25 °C and a T_g of 82 °C for ELO cured with citric acid.^[15] Altuna et al. achieved a T_g of 30 °C for a 100% bio-based thermoset based on epoxidized soybean oil.^[32] Qi et al. cured ESO with tannic acid and found a maximum T_g of 77 °C and a storage modulus of 1103 MPa at 25 °C.^[5] Previous research showed that high T_g could be obtained with ELO. However, petroleum-based curing agents were used. Todorovic et al. for example found a T_g of 145 °C for ELO cured with the petroleum-based methyltetrahydrophthalic anhydride (MTHPA) hardener.^[15] This underlines the capacity of TA to create a stiff network due to its highly aromatic structure and compete with standard petroleum-based hardeners.

3.3. Mechanical Properties

Because epoxy thermosets are subjected to flexural loading in typical applications, flexural testing is a relevant mechanical test and determines the flexural properties (flexural strength, flexural modulus, and elongation at break). The average flexural modulus, flexural strength, and elongation at break obtained for the TA/ELO samples cured with C1 and C2 are summarized in Table 3.

Flexural modulus and flexural strength are increasing when the curing condition C2 instead of C1 is applied as the material becomes stiffer and more resilient to flexural load due to higher cross-linking of the polymer chains.

As for the storage modulus, the flexural modulus increases with the amount of TA added to ELO. High stiffness is needed in high-performance applications. A maximum flexural modulus of 2986 MPa was obtained for the sample TA/ELO 2.0 cured with C2. Therefore, the fully bio-based TA/ELO thermoset can reach similar stiffness under flexural load to high-performance commercial petroleum-based epoxy materials. As a comparison, the CR80 epoxy system from SIKA is an epoxy resin system suitable for producing high-performance fiber-reinforced composites for marine, wind turbine, and general industrial composite areas. After complete cure, CR80 reaches a flexural modulus of 2900–2950 MPa.^[33]

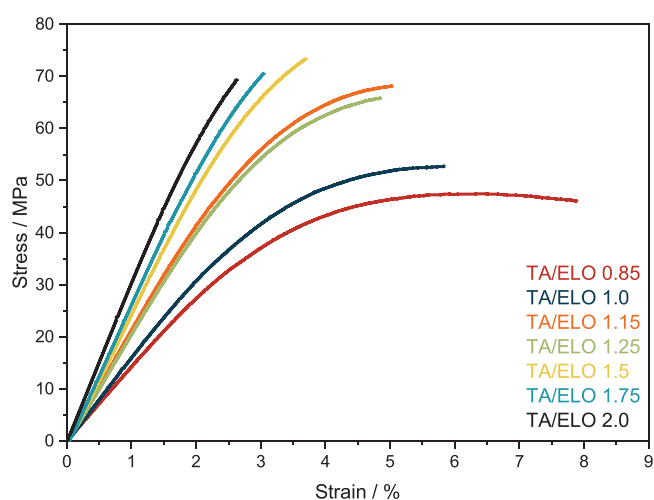


Figure 7. Representative stress–strain curves for the different TA/ELO samples cured with C2.

The increase of the stiffness with the –OH/epoxide molar ratio leads to a brittle behavior as the elongation at break decreases (Table 3). The samples TA/ELO 0.85, 1.0, and 1.15 cured with C1 present a high uncertainty on the elongation at break. We believe that due to poor curing efficiency, cross-linking and hence stiffness along the sample was inhomogeneous, resulting in a random flexural-load deflection. Figure 7 shows representative stress/strain curves obtained for the TA/ELO samples cured with C2. The flexural strength reaches its optimum (72 MPa) with TA/ELO 1.5 cured with C2. Being able to modulate the flexural properties by varying the TA amount inside ELO is of great interest. It enables the bio-based epoxy to be used in various applications as the TA/ELO thermoset can be turned into a very stiff and brittle material as well as a flexible material with a high flexural load-deflection before breakage.

3.4. Thermal Stability

The curing regime C2 allows higher T_g and stiffness and is more suited for obtaining a high-performance thermoset. Therefore, only the thermal stabilities under nitrogen of the TA/ELO samples cured with C2 were investigated via thermogravimetric

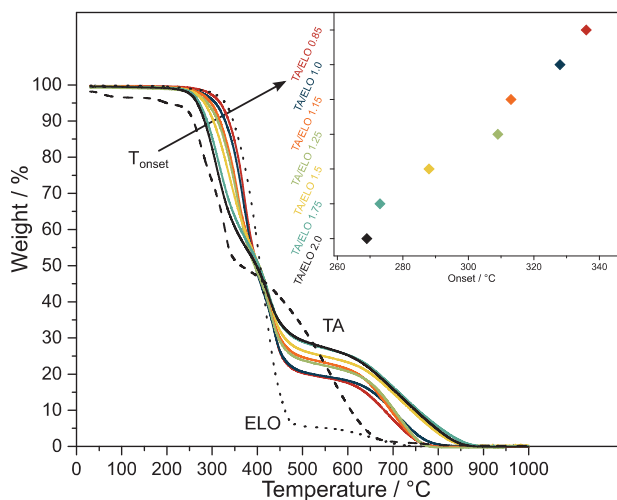


Figure 8. TGA curves of the TA/ELO samples cured with C2 and of pure ELO (dotted) and milled TA (dashed) and respective temperature of 5% weight loss ($T_{5\%}$).

analysis (TGA). As expected, an excess of TA affects the thermal stability of the TA/ELO thermoset, particularly for TA/ELO 1.75 and 2.0, as a high amount of unreacted TA that did not crosslink is present in the matrix. Thus, with an increasing TA content, the $T_{5\%}$ of the thermoset approaches the $T_{5\%}$ of neat TA, which is found to be roughly at 235 °C (Figure 8).

For samples containing a small amount of TA, especially TA/ELO 0.85 and 1.0, similar TGA curves to standard commercially available high-performance epoxy are obtained. Figure S11 (Supporting Information) depicts the TGA curve of TA/ELO 0.85 and the high-performance epoxy CR80 from SIKA. Even if the increasing amount of TA impacts the thermal stability of the thermoset negatively, the $T_{5\%}$ of TA/ELO 2.0 at 267 °C is high enough to not degrade the material under usage in standard applications.

3.5. Sample Morphology

The morphology of the fracture surfaces after flexural testing was investigated in Figure 9. Three different TA/ELO samples cured

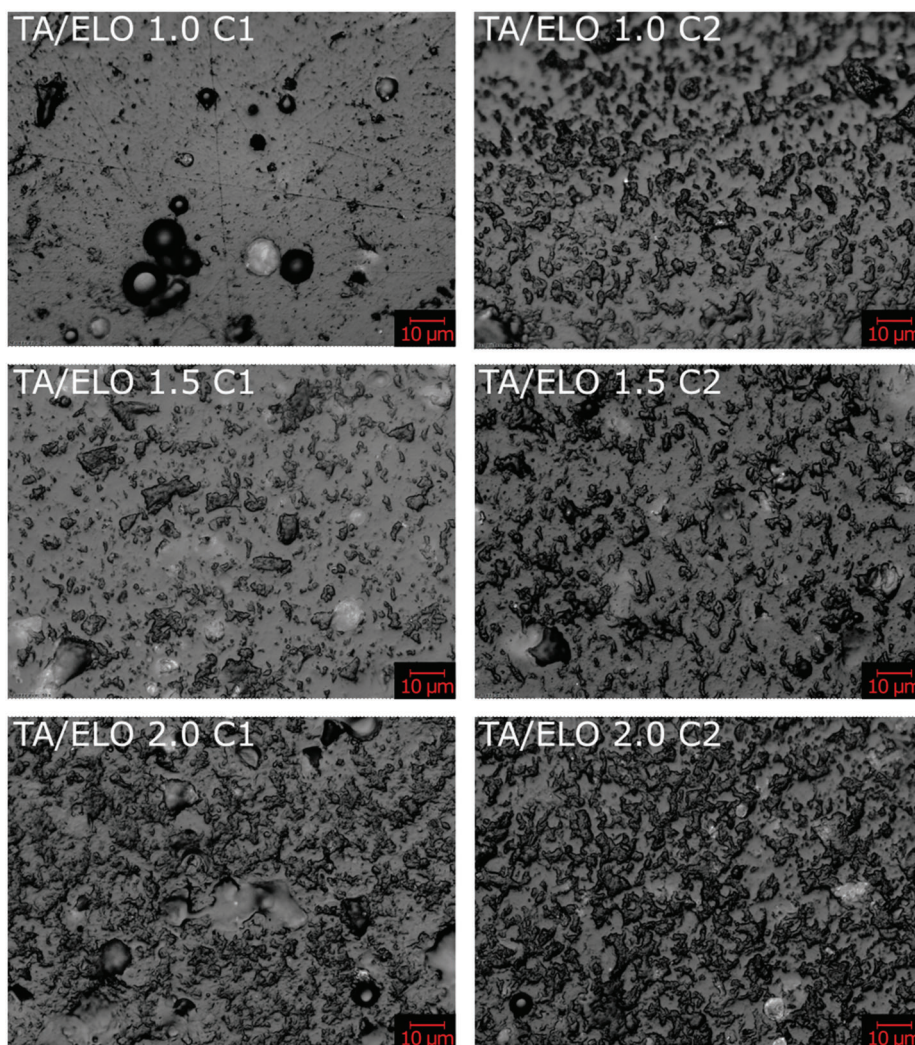


Figure 9. Representative microscope images of the fracture surface of TA/ELO 1.0, 1.5, and 2.0 cured with C1 and C2 after flexural testing.

with C1 and C2 were chosen to see the impact of the curing temperature and the amount of TA (equimolar amount: TA/ELO 1.0; excess of TA: TA/ELO 1.5 and high excess of TA: TA/ELO 2.0) on the morphology of the sample.

Black spots with a circular shape can be spotted on all surfaces analyzed. Due to the high viscosity of the TA/ELO mixture, some voids are present in the material. The surface of TA/ELO 1.0 cured with C1 is rather smooth whereas a rough surface can be observed with the curing condition C2. With a very high amount of TA (TA/ELO 1.5 and 2.0), a rough surface is already observed with curing condition C1 and the roughness becomes more striking with C2. We believe that this rough surface is a result of the cross-linking reaction between ELO and TA that takes place mainly with hydroxyl groups on the surface of the milled TA particles leaving the inner core unreacted. As already highlighted previously, with an excess of TA, a higher cross-linking can be achieved, and curing with C2 allows further cross-linking. It is obvious that, when added in excess, all the TA particles cannot react with ELO, leading to a composite-like structure. Even though the excess of TA is responsible for a higher cross-linking, the Soxhlet degree of cross-linking is decreasing when the amount of TA increases in the material, showing that there is a clear increasing amount of unreacted TA in the material (Figure S7, Supporting Information). The presence of unreacted TA particles in the epoxy after curing could also be highlighted with the water absorption test. Due to the hydrophilic nature of TA, the water absorption of TA/ELO epoxy increases with the TA amount in the material, as more TA particles remain unreacted in the cured material (Figure S12, Supporting Information).

4. Conclusion

EVOs are known to have drawbacks. Their inherently aliphatic nature and the absence of a stiff and aromatic structure strongly limit the practical use in structural applications, and rather poor mechanical and thermal properties are reported in the literature for EVO-based epoxies. However, this study shows that TA is an outstanding curing agent for ELO as a similar flexural modulus (2986 MPa) to commercial petroleum-based epoxy materials, a high T_g (147 °C) and flexural strength (72 MPa) could be obtained. Its high degree of rigidity and aromatic structure contributes to the high thermal and mechanical properties of the TA/ELO thermoset. With the particle size of TA significantly reduced by a two-step milling procedure, TA can disperse homogeneously without using solvents in ELO to obtain a fully bio-based thermoset with good material characteristics.

Due to the steric hindrance and the low reactivity of the phenol groups, a high amount of TA and curing of the thermoset 16 h at 120 °C + 3 h at 140 °C favors the cross-linking and the obtention of stiff material with a high T_g . An excess of TA negatively affects the thermal stability of the thermoset. Nevertheless, the starting temperature of degradation allows usage in most common applications.

The strong thermal and mechanical properties obtained for the fully bio-based TA/ELO thermoset make it a serious alternative to petroleum and Bisphenol-A-based epoxy for high-performance applications. Future work will be dedicated to the optimization of the curing process and the production of composites. Catalysts, preferably bio-based, will be introduced in the TA/ELO mixture

to accelerate the curing process and make it more adapted for industrial purposes. The developed thermoset will then be reinforced with various fibers to determine the properties of the formed composites.

Supporting Information

Supporting Information is available from the Wiley Online Library or from the author.

Acknowledgements

N.R. and J.M.B. contributed equally to this work. The authors want to thank Jesús Bendala de Orbe and Hongwu Zhang for their help with the sample preparation. The authors also want to thank Hanh My Bui for the help with particle size determination. The funding by the German Federal Ministry of Education and Research (BMBF) for the "Green Carbon" project (FKZ: 03SF0577A) is gratefully acknowledged.

Open access funding enabled and organized by Projekt DEAL.

Conflict of Interest

The authors declare no conflict of interest.

Data Availability Statement

The data that support the findings of this study are available from the corresponding author upon reasonable request.

Keywords

bio-based materials, epoxidized linseed oil, epoxidized vegetable oils, epoxy thermoset, tannic acid

Received: July 7, 2022
Revised: August 19, 2022
Published online: October 3, 2022

- [1] Expert market research, <https://www.expertmarketresearch.com/reports/epoxy-resins-market> (accessed: October 2022).
- [2] E. A. Baroncini, S. Kumar Yadav, G. R. Palmese, J. F. Stanzione, *J. Appl. Polym. Sci.* **2016**, *133*, 44103.
- [3] a) K. Hąc-Wydro, K. Połec, M. Broniatowski, *J. Mol. Liq.* **2019**, *289*, 111136; b) K.-A. Hwang, K.-C. Choi, in *Advances in Molecular Toxicology* (Eds: J. C. Fishbein, J. M. Heilman), Elsevier, MA, USA **2015**; c) R. A. Nowak, F. Koohestani, J. Bi, P. Mehrotra, F. S. Mesquita, F. Masoud, S. A. Machado, *Comprehensive Toxicology (Second Edition)*, **2010**, 499, <https://doi.org/10.1016/B978-0-08-046884-6.01130-1>; d) M. N. Saleh, N. Z. Tomić, A. Marinković, S. Teixeira De Freitas, *Polym. Test.* **2021**, *96*, 107122; e) J. S. Terry, A. C. Taylor, *J. Appl. Polym. Sci.* **2021**, *138*, 50417; f) R. Wang, T. Schuman, in *Green Materials from Plant Oils*, The Royal Society of Chemistry, Cambridge, USA **2015**; g) H. Feng, J. Hu, D. Jin, S. Wang, J. Dai, X. Liu, *Acta Polym. Sin.* **2022**, *2022*, 1; h) J. Liu, S. Wang, Y. Peng, J. Zhu, W. Zhao, X. Liu, *Progress in Polymer Science.* **2021**, *113*, 101353.
- [4] M. R. Loos, L. A. F. Coelho, S. H. Pezzin, S. C. Amico, *Polímeros.* **2008**, *18*, 76.

- [5] M. Qi, Y.-J. Xu, W.-H. Rao, X.i Luo, L.i Chen, Y.u-Z. Wang, *RSC Adv.* **2018**, *8*, 26948.
- [6] M. Korey, G. P. Mendis, J. P. Youngblood, J. A. Howarter, *J. Polym. Sci. A Polym. Chem.* **2018**, *56*, 1468.
- [7] Y.i Li, F. Xiao, K.-S. Moon, C. P. Wong, *J. Polym. Sci. A Polym. Chem.* **2006**, *44*, 1020.
- [8] a) S. M. Danov, O. A. Kazantsev, A. L. Esipovich, A. S. Belousov, A. E. Rogozhin, E. A. Kanakov, *Catal. Sci. Technol.* **2017**, *7*, 3659; b) N.w Manthey, F. Cardona, G. Francucci, T. Aravinthan, *J. Compos. Mater.* **2014**, *48*, 1611; c) R. Mustapha, A. R. Rahmat, R. Abdul Majid, S. N. H. Mustapha, *Polym. -Plast. Technol. Mater.* **2019**, *58*, 1311; d) T. S. Omonov, J. M. Curtis, *J. Appl. Polym. Sci.* **2014**, *131*, <https://doi.org/10.1002/app.40142>; e) S. G. Tan, W. S. Chow, *J Am. Oil Chem. Soc.* **2011**, *88*, 915.
- [9] Q. Ma, X. Liu, R. Zhang, J. Zhu, Y. Jiang, *Green Chem.* **2013**, *15*, 1300.
- [10] M. D. Samper, R. Petrucci, L. Sánchez-Nacher, R. Balart, J. M. Kenny, *Compos. B. Eng.* **2015**, *71*, 203.
- [11] E. Ramon, C. Sguazzo, P. Moreira, *Aerospace.* **2018**, *5*, 110.
- [12] R. Wang, *Dissertation*, Missouri University of Science and Technology, Missouri **2014**.
- [13] N. R. Paluvai, S. Mohanty, S. K. Nayak, *Polym. Plast. Technol. Eng.* **2014**, *53*, 1723.
- [14] a) N. Boquillon, C. Fringant, *Polymer.* **2000**, *41*, 8603; b) J.-M. Pin, N. Sbirrazzuoli, A. Mija, *ChemSusChem.* **2015**, *8*, 1232.
- [15] A. Todorovic, K. Resch-Fauster, A. R. Mahendran, G. Oreski, W. Kern, *J. Appl. Polym. Sci.* **2021**, *138*, 50239.
- [16] US Food and Drug Administration (FDA), <https://www.ecfr.gov/current/title-21/chapter-I/subchapter-B/part-184/subpart-B/section-184.1097> (accessed: January 2022).
- [17] Y.-O. Kim, J. Cho, H. Yeo, B. W. Lee, B. J. Moon, Y.-M. Ha, Y. R. Jo, Y. C. Jung, *ACS Sustain. Chem. Eng.* **2019**, *7*, 3858.
- [18] M. Shibata, K. Nakai, *J. Polym. Sci. B Polym. Phys.* **2010**, *48*, 425.
- [19] X. Feng, J. Fan, A. Li, G. Li, *ACS Sustain. Chem. Eng.* **2020**, *8*, 874.
- [20] M. Shibata, N. Teramoto, K. Makino, *J. Appl. Polym. Sci.* **2011**, *120*, 273.
- [21] a) C. Yi, P. Rostron, N. Vahdati, E. Gunister, A. Alfantazi, *Prog. Org. Coat.* **2018**, *124*, 165; b) O. Vryonis, T. Andritsch, A. S. Vaughan, P. L. Lewin, *IEEE Conference on Electrical Insulation and Dielectric Phenomenon (CEIDP).* **2017**, 509, <https://doi.org/10.1109/CEIDP.2017.8257525>; c) K. Qiu, R. Tannenbaum, K. I. Jacob, *Polym. Eng. Sci.* **2021**, *61*, 1281; d) S.-G. Hong, C.-S. Wu, *Thermochim. Acta* **1998**, *316*, 167.
- [22] P. J. Gay, *J. Soc. Chem. Ind.* **1933**, *52*, 703.
- [23] L. Shechter, J. Wynstra, *Ind. Eng. Chem.* **1956**, *48*, 86.
- [24] D. Lascano, L. Quiles-Carrillo, S. Torres-Giner, T. Boronat, N. Montanes, *Polymers.* **2019**, *11*, 1354.
- [25] S. Ebnesajjad, *Surface Treatment of Materials for Adhesive Bonding*, 2nd ed. William Andrew, Norwich **2014**.
- [26] a) M. R. M. Hafezal, A. Khalina, Z. A. Zurina, M.d D. M. Azaman, Z. M. Hanafee, *J. Compos. Sci.* **2019**, *3*, 6; b) A. Campanella, M. Zhan, P. Watt, A. T. Grous, C. Shen, R. P. Wool, *Compos. – A: Appl. Sci. Manuf.* **2015**, *72*, 192.
- [27] F. C. Fernandes, K. Kirwan, P. R. Wilson, S. R. Coles, *Green Mater.* **2018**, *6*, 38.
- [28] J. Lange, N. Altmann, C. Kelly, P. Halley, *Polymer.* **2000**, *41*, 5949.
- [29] N. Ghasemi Rad, Z. Karami, M. J. Zohuriaan-Mehr, A. Salimi, K. Kabiri, *Polym. Adv. Technol.* **2019**, *30*, 2361.
- [30] a) A. Hale, C. W. Macosko, H. E. Bair, *Macromolecules* **1991**, *24*, 2610; b) A. Shefer, M. Gottlieb, *Macromolecules.* **1992**, *25*, 4036.
- [31] A. Shrivastava, *Introduction to Plastics Technology*, William Andrew, Saint Louis **2018**.
- [32] F. I. Altuna, V. Pettarin, R. J. J. Williams, *Green Chem.* **2013**, *15*, 3360.
- [33] Sika Deutschland, GmbH, <https://industry.sika.com/content/dam/dms/global-industry/m/Biresin-CR80-SikaBiresin-CH80-2-New.pdf> (accessed: January 2022).